



Discovery of novel 4-amino-6-arylaminopyrimidine-5-carbaldehyde oximes as dual inhibitors of EGFR and ErbB-2 protein tyrosine kinases

Guozhang Xu*, Lily Lee Searle, Terry V. Hughes, Amanda K. Beck, Peter J. Connolly, Marta C. Abad, Michael P. Neeper, Geoffrey T. Struble, Barry A. Springer, Stuart L. Emanuel, Robert H. Gruninger, Niranjana Pandey, Mary Adams, Sandra Moreno-Mazza, Angel R. Fuentes-Pesquera, Steven A. Middleton, Lee M. Greenberger

Johnson & Johnson Pharmaceutical Research & Development, Medicinal Chemistry, 8 Clarke Drive, Cranbury, NJ 08512, USA

ARTICLE INFO

Article history:

Received 24 April 2008

Accepted 7 May 2008

Available online 10 May 2008

Keywords:

Receptor tyrosine kinase

ErbB-2

EGFR

Oxime

Quinazoline

Bioisostere

ABSTRACT

We herein disclose a novel series of 4-aminopyrimidine-5-carbaldehyde oximes that are potent and selective inhibitors of both EGFR and ErbB-2 tyrosine kinases, with IC_{50} values in the nanomolar range. Structure–activity relationship (SAR) studies elucidated a critical role for the 4-amino and C-6 arylamino moieties. The X-ray co-crystal structure of EGFR with **37** was determined and validated our design rationale.

© 2008 Elsevier Ltd. All rights reserved.

The epidermal growth factor (ErbB) family of receptor tyrosine kinases (RTKs) plays an important role in the regulation of cell growth, differentiation, and survival.¹ The ErbB family consists of four receptors: epidermal growth factor receptor (EGFR or ErbB-1), ErbB-2 (Her-2), ErbB-3, and ErbB-4.² Dysregulation of the ErbB signaling pathways has been observed in numerous solid tumors (e.g., breast, lung, colon, and prostate).³ The increased ErbB signaling observed in these tumors usually results from receptor overexpression, gene amplification, mutation, and/or elevated levels of ErbB ligands. Both EGFR and ErbB-2 have been targeted for inhibitor development by the pharmaceutical industry,⁴ and over a decade of research has culminated in the approval of gefitinib **1** and erlotinib **2** for the treatment of non-small cell lung cancer following prior chemotherapeutic intervention (Fig. 1).⁵ Lapatinib **3**, a potent dual EGFR/ErbB-2 inhibitor, for the treatment of advanced or metastatic ErbB-2 positive breast cancer is currently in Phase II and III trials for the treatment of other solid tumors.⁶ These agents belong to the 4-anilinoquinazoline class of inhibitors and the key features between the receptor and this template have been revealed as follows.^{7,8} (1) The quinazoline moiety fits into the ATP binding pocket of the kinase domain, where the N-1 nitrogen of the quinazoline nucleus interacts with the backbone NH of Met-

769 via a hydrogen bond, and a water mediated hydrogen bonding is observed between the N-3 of the quinazoline and the Thr-766 side chain. (2) The aniline ring fills an adjacent lipophilic pocket. (3) The solubilizing side chains at C-6 and/or C-7 of the quinazoline core act to improve physical properties and confer a more favorable pharmacokinetic profile.

We envisioned that replacement of the quinazoline found in molecules like **1**, **2**, and **3** with our recently reported 4-aminopyrimidine-5-carbaldehyde oxime scaffold^{9,10} could lead to the identification of potent EGFR/ErbB-2 dual inhibitors (Fig. 2). The *pseudo* six-membered ring formed by the intramolecular NH...N=C hydrogen bond of **5** would function as a mimic of the phenyl ring of the quinazoline. In this report, we describe the synthesis and structure–activity relationship (SAR) of a novel series of dual EGFR/ErbB-2 inhibitors designed around this hypothesis. An X-ray co-crystal structure of a representative compound in complex with EGFR is also described.

Synthesis of the target molecules is illustrated in Scheme 1. Treatment of 4,6-dichloropyrimidine-5-carboxaldehyde¹¹ **6** with either NH_3 gas or CH_3NH_2 in toluene gave **7**, followed by reaction with an appropriately substituted aniline to give pyrimidine-5-carboxaldehyde **8**. High conversion of **7**→**8** was usually achieved when the base (DIEA) was added first and the aniline was added last. Reversal of the order of addition sometimes resulted in the Schiff base formation with the C-5 aldehyde

* Corresponding author. Tel.: +1 609 655 6915; fax: +1 609 655 6930.

E-mail address: gxu4@prdus.jnj.com (G. Xu).

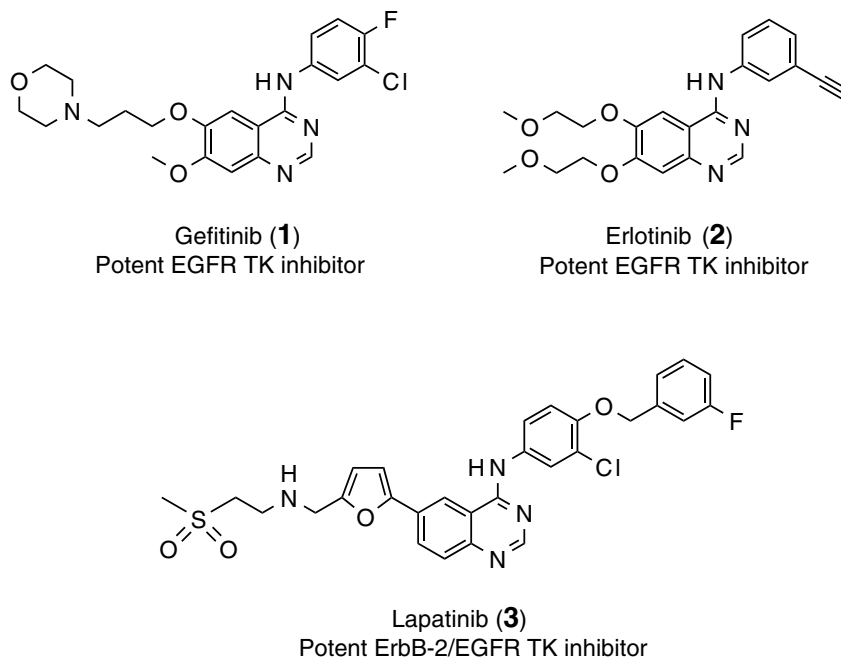


Figure 1. Examples of EGFR and ErbB-2 receptor tyrosine kinase inhibitors in clinical use: Gefitinib **1**; Erlotinib **2**; Lapatinib **3**.

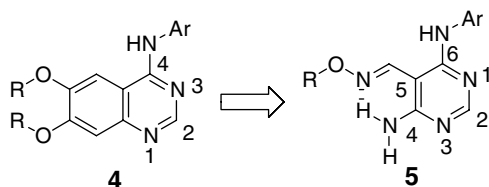


Figure 2. Quinazoline and 4-amino-6-arylamino-5-carbaldehyde oxime templates.

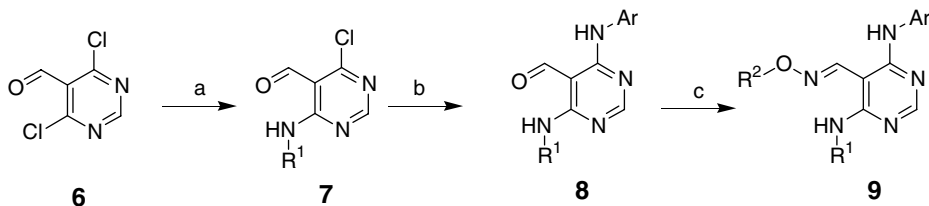
moiety. Subsequent condensation of **8** with an O-substituted hydroxylamine provided the desired pyrimidine oxime **9**. It should be pointed out that the *E*-isomer was either the major or exclusive product obtained.

Anilines used to prepare analogues **20–24**, **26** and **27** were synthesized by published procedures.^{12,13} Aniline **12** required for the synthesis of analogue **30** was prepared according to Scheme 2. Pd/C-catalyzed reaction of 2-iodophenol **10** with 1-ethynyl-3-fluoro-

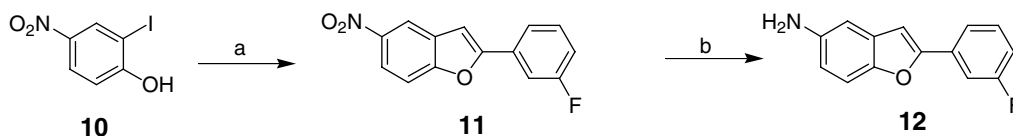
benzene in the presence of PPh₃, CuI, and prolinol afforded 2-substituted benzo[*b*]furan **11**,¹⁴ which was reduced to **12** via hydrogenation.

To ascertain whether the 4-aminopyrimidine-5-carboxaldehyde oxime derivatives were capable of affording potent EGFR/ ErbB-2 inhibition, we selected the 1-(3-fluorobenzyl)indazol-5-amino group as the C-6 side chain since it has been shown in both pyrrolotriazine¹⁵ and quinazoline¹⁶ scaffolds to provide optimal dual EGFR and ErbB-2 kinase inhibitions. We were delighted to find that compound **13** (Table 1) displayed potent inhibition against both EGFR and ErbB-2 with IC₅₀ = 8 and 12 nM, respectively.¹⁷ However, methyl substitution of the C-4 amino group (**14**) abrogated both EGFR and ErbB-2 activities. Such a pronounced drop in activity against the enzyme suggested that C-4 NH₂ is necessary for binding, or that the methyl group prevents the molecule from attaining a proper conformation for binding to the enzyme.

We next turned our attention to determining the effect of various modifications at the C-6 aniline position on EGFR and ErbB-2

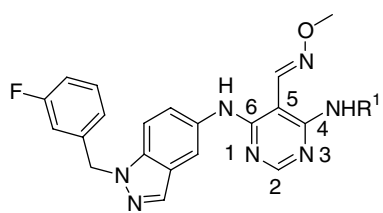


Scheme 1. Reagents and conditions: (a) R¹-NH₂, toluene (90%); (b) DMSO, DIEA, Ar-NH₂, 100 °C (65–80%); (c) R²-ONH₂·HCl, MeOH, 75 °C (70–90%).



Scheme 2. Reagents and conditions: (a) 1-ethynyl-3-fluoro-benzene, 10% Pd/C, PPh₃, CuI, *s*-prolinol/H₂O (80%); (b) H₂, 5% Pd/C (95%).

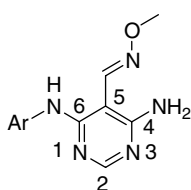
Table 1
Structure–activity relationships for the C-4 position



Compound	R ₁	EGFR IC ₅₀ ^a (μM)	ErbB-2 IC ₅₀ ^a (μM)
13	H	0.008	0.012
14	CH ₃	(48% inh at 2 μM)	(39% inh at 10 μM)

^a Mean values of at least three experiments are used for enzyme assays of ErbB-2/EGFR, IC₅₀ values reported as μM concentrations. See Ref. ¹⁷ for assay conditions.

Table 2
Structure–activity relationships for the C-6 aniline substitution



Compound	Ar	EGFR IC ₅₀ ^a (μM)	ErbB-2 IC ₅₀ ^a (μM)
15	(3-Cl-4-F)phenyl	0.070	0.204
16	3-Br-phenyl	0.024	0.557
17	(3-Cl-4-F)benzyl	1.123	5.22
18	Indazol-5-yl	0.306	4.123
19	1-benzyl-indazol-5-yl	0.044	0.022
20	1-(3-Cl-benzyl)indazol-5-yl	0.023	0.030
21	1-(3-CN-benzyl)indazol-5-yl	0.020	0.044
22	1-(3-OCH ₃ -benzyl)indazol-5-yl	0.267	NT ^b
13	1-(3-F-benzyl)indazol-5-yl	0.008	0.012
23	3-Cl-4-(3,5-F ₂ -benzyloxy)phenyl	0.033	(52% inh at 10 μM)
24	1-(4-F-benzyl)indazol-5-yl	0.104	0.189
25	1-(3-F-benzyl)indol-5-yl	0.013	0.027
26	2-(3-F-benzyl)benzoimidazol-5-yl	0.048	0.076
27	1-(3-F-benzyl)-2,3-dihydro-indol-5-yl	0.057	0.255
28	(3-Cl-4-benzyloxy)phenyl	0.016	0.153
29	3-Cl-4-(3-F-benzyloxy)phenyl	0.012	0.018
30	2-(3-F-phenyl)benzofuran-5-yl	(<10% inh at 2 μM)	(<10% inh at 10 μM)

^a Mean values of at least three experiments are used for enzyme assays of ErbB-2/EGFR.

^b Not tested.

kinase inhibitory activities (Table 2). Analogues with small C-6 anilines (**15** and **16**) or simple fused 5,6-bicyclic heterocycles (**18**) were selective EGFR inhibitors. However, this activity was dramatically decreased if the aromatic ring was displaced by one carbon (**17**). Appending a lipophilic benzyl group (**19**) to the C-6 indazolylamine increased ErbB-2 kinase inhibition without reducing EGFR potency. A similar trend was also reported in the quinazoline series where increasing size at the C-4 aniline position substantially improved ErbB-2 activity.¹⁸ Both *m*-chlorobenzyl (**20**) and *m*-cyanobenzyl (**21**) analogues showed comparable potency to compound **19**. Interestingly, adding a fluorine atom at the 3-position of the benzyl group (**13**) resulted in a 5-fold increase in inhibitory potency against EGFR and an approximate 2-fold increase against ErbB-2, highlighting the potential interaction of fluorine with the enzyme (*vide infra*). There was slight increase in EGFR potency for the 3,5-difluorobenzyl compound **23**. However, larger groups

such as methoxy at the 3-position (**22**) exhibited greatly reduced potency against EGFR. The 4-fluorobenzyl analogue **24** also proved to have suboptimal potency. Indole-substituted analogue **25** maintained potency against both enzymes, whereas the 2,3-dihydro-indole compound **27** showed much weaker potency against EGFR and ErbB-2. Changing the indazole group to benzoimidazole (**26**), which also displaces the 3-fluorobenzyl group to the 2-position of the heterocycle, resulted in 6-fold lower potency against both enzymes. Alternative extended anilines (**28** and **29**) gave comparable, high EGFR potency but different selectivity versus ErbB-2. The benzofuran analogue **30**, which may be viewed as a conformationally restricted version of **29**, was inactive in both EGFR and ErbB-2 assays.

To study the SAR at the oxime side chain (R² group), a series of unsubstituted and *O*-alkyl oximes were prepared and tested. The inhibitory activity of the resultant compounds is listed in Table 3. In general, all modifications led to potent activity against EGFR. However, compounds with bulky and hydrophobic substituents (**33**, **35**, and **36**) are less potent in the ErbB-2 assay. The cellular activity of these compounds was evaluated in proliferation assays using the SKBR3 and BT474 cell lines,¹⁹ both of which overexpress ErbB-2. Compounds **13**, **32**, **34**, **35**, and **36** showed submicromolar cellular antiproliferative potency, whereas compound **31** had reduced activity even at 10 μM, suggesting that it does not penetrate the cell membrane effectively.

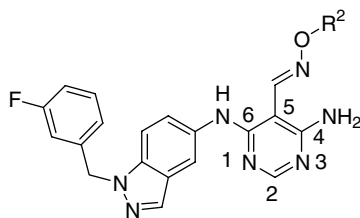
In order to determine the kinase selectivity for this series, compounds **25** and **28** were evaluated against a panel of 102 kinases at the concentration of 3 μM in the presence of 100 μM ATP²⁰ and found to be highly selective for the EGFR subfamily. In pharmacokinetic evaluation in Sprague–Dawley rats, compound **28** exhibited high plasma levels, low volume of distribution, and low clearance (Table 4). Its bioavailability is 15%.

To further validate our design rationale, an X-ray crystal structure of EGFR with compound **37** bound at the ATP site was solved at a resolution of 2.3 Å.²¹ Figure 3 illustrates the complex and shows that the pyrimidine ring nitrogen N3 interacts with the backbone NH of Met793 in the kinase hinge region, whereas the amino group at the C-4 position is engaged in a second hydrogen bond with the backbone C=O of Met793. This binding mode explains the finding that *N*-methylation at C-4 amino position was detrimental for activity. The 1-(3-fluorobenzyl)indazolylamino group is oriented deep in the back of the ATP binding site and makes predominantly hydrophobic interactions with the protein. The 3-fluorobenzyl group occupies a pocket formed by the side chains of Met766, Leu777, Thr790, Thr854, and Phe856. The 3-fluoro on the benzyl group is hydrogen bonded to both backbone NH groups of Arg776 and Thr790, and is important for optimally potent inhibition of EGFR. This also explains why replacement by chlorine, cyano, or methoxy group resulted in less potent compounds (**20**, **21**, and **22**), because they cannot occupy this binding pocket without displacing key residues. The N-2 atom of the indazole ring forms a weak hydrogen bond to the backbone C=O of Leu 788 (3.7 Å). The aniline nitrogen and the N-1 atom of the indazole ring are not involved in any direct hydrogen bonding interactions with the protein. The methoxyethoxy moiety appended to the oxime is extended to the solvent region, which supports the finding that most of the analogues with alkyl oxime substituents give favorable inhibitory potency against both EGFR and ErbB-2. The C-4 amino group forms an intramolecular hydrogen bond with the oxime nitrogen atom as we anticipated, therefore mimicking the quinazoline *phenyl* ring.

In summary, 4-amino-6-arylamino-pyrimidine-5-carbaldehyde oxime derivatives showed potent inhibition of ErbB-2/EGFR kinase activities and antiproliferative effects toward ErbB-2 overexpressing SK-BR-3 and BT474 cell lines. An unsubstituted amino group at the C-4 position is essential for potent inhibitory

Table 3

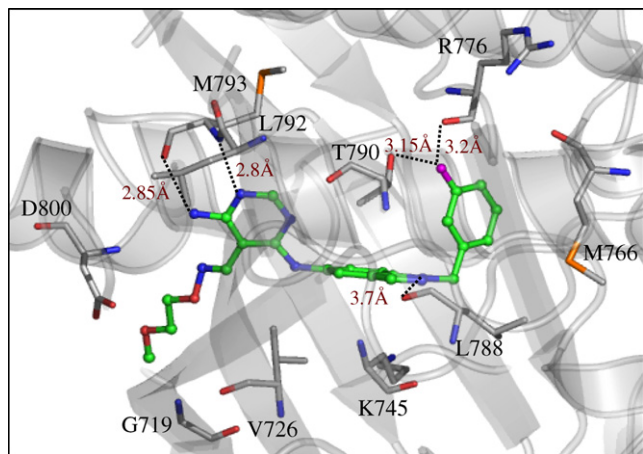
Structure–activity relationships for the C-5 side chain



Compound	R ₂	EGFR IC ₅₀ ^a (μM)	ErbB-2 IC ₅₀ ^a (μM)	SKBR3 IC ₅₀ ^a (μM)	BT474 IC ₅₀ ^a (μM)
13	CH ₃	0.008	0.012	0.26	0.25
31	H	0.012	0.042	(41% inh at 10 μM)	(34% inh at 10 μM)
32	CH ₂ CH ₃	0.005	0.007	0.27	0.062
33	CH ₂ CH(CH ₃) ₂	0.032	0.173	1.88	1.03
34	CH(CH ₃) ₂	0.014	0.025	0.71	0.54
35	benzyl	0.023	0.095	0.18	0.13
36	2-OCH ₃ -benzyl	0.047	0.435	0.13	0.21
37	(CH ₂) ₂ OCH ₃	0.014	0.006	(84% inh at 10 μM)	(60% inh at 10 μM)

^a Mean values of at least three experiments are used for enzyme assays of ErbB-2/EGFR, IC₅₀ values reported as μM concentrations.**Table 4**Pharmacokinetic parameters for compound **28**, determined after dosing to Sprague–Dawley rats at 2 mg/kg iv (vehicle = 10% solutol in D5W) and 10 mg/kg po (vehicle = 0.5% hydroxypropyl methylcellulose)

Compound	V _{dss} (L/Kg)	Cl (ml/min/Kg)	po C _{max} (μM)	po T _{max} (h)	po T _{1/2} (h)	po AUC (μM.h)	Bioavailability %
28	0.17	3.56	5.7	0.63	8.4	19.3	15

**Figure 3.** Interactions between EGFR and compound **37**. Compound **37** is shown in green, protein residues are colored gray and atoms are colored by element for both molecules with nitrogen blue, oxygen red and fluorine light green.

activity. This result was supported by the X-ray crystallographic elucidation of the complex of **37** with EGFR, where the NH₂ made key hydrogen bonding interaction with backbone C=O of Met 793. The C-6 aniline portion determines the potency and kinase selectivity, and this conclusion parallels the literature SAR at the C-4 aniline position reported for quinazoline-based RTK inhibitors.^{22,23} The oxime side chain is oriented toward the solvent front, consistent with the observation that a variety of substituents were tolerated. These studies suggest that 4-amino-6-arylaminopyrimidine-5-carbaldehyde oxime scaffold effectively mimics the well-known quinazoline kinase template. Future reports will detail the design of potent dual EGFR/ErbB-2 inhibitors with improved bioavailability that demonstrate antitumor efficacy in preclinical disease models.

Acknowledgment

Use of the IMCA-CAT beamline 17-ID (or 17-BM) at the Advanced Photon Source was supported by the companies of the Industrial Macromolecular Crystallography Association through a contract with the Center for Advanced Radiation Sources at the University of Chicago.

References and notes

- Olayioye, M. A.; Neve, R. M.; Lane, H. A.; Hynes, N. E. *EMBO J.* **2000**, *19*, 3159.
- (a) Salomon, D. S.; Bradt, R.; Ciardiello, F.; Normanno, N. *Crit. Rev. Oncol. Hematol.* **1995**, *19*, 183; (b) Black, J. D.; Brattain, M. G.; Krishnamurthi, S. A.; Dawson, D. M.; Willson, J. K. *Curr. Opin. Invest. Drugs* **2003**, *4*, 1451.
- (a) Gullick, W. J. *Br. Med. Bull.* **1991**, *47*, 87; (b) Woodburn, J. R. *Pharmacol. Ther.* **1999**, *82*, 241.
- Seymour, L. *Curr. Opin. Invest. Drugs* **2003**, *4*, 658.
- (a) Baselga, J.; Tripathy, D.; Mendelsohn, J.; Baughman, S.; Benz, C. C.; Dantis, L.; Sklarin, N. T.; Seidman, A. D.; Hudis, C. A.; Moore, J.; Rosen, P. P.; Twaddell, T.; Henderson, I. C.; Norton, L. *J. Clin. Oncol.* **1996**, *14*, 737; (b) Waksal, H. W. *Cancer Metastasis Rev.* **2000**, *18*, 427; (c) Gschwind, A.; Fisher, O. M.; Ullrich, A. *Nature* **2004**, *361*.
- Rusnak, D. W.; Lackey, K.; Affleck, K.; Wood, E. R.; Alligood, K. J.; Rhodes, N.; Keith, B. R.; Murray, D. M.; Knight, W. B.; Mullin, R. J.; Gilmer, T. M. *Mol. Cancer Ther.* **2001**, *1*, 85.
- Stamo, J.; Sliwkowski, M. X.; Eigenbrot, C. J. *J. Biol. Chem.* **2002**, *277*, 46265.
- Liao, J. J. *Med. Chem.* **2007**, *50*, 409.
- Huang, S.; Li, R.; Connolly, P. J.; Xu, G.; Gaul, M. D.; Emanuel, S. L.; LaMontagne, K. R.; Greenberger, L. M. *Bioorg. Med. Chem. Lett.* **2006**, *16*, 6063.
- Gaul, M. D.; Xu, G.; Kirkpatrick, J.; Ott, H.; Baumann, C. A. *Bioorg. Med. Chem. Lett.* **2007**, *17*, 4861.
- Gomtsyan, A.; Didomenico, S.; Lee, C.; Matulenko, M. A.; Kim, K.; Kowaluk, E. A.; Wismer, C. T.; Mikusa, J.; Yu, H.; Kohlhaas, K.; Jarvis, M. F.; Bhagwat, S. S. *J. Med. Chem.* **2002**, *45*, 3639.
- Tsou, H.; Overbeek-Klumpers, E.; Hallett, W.; Reich, M.; Floyd, M. B.; Johnson, B. D.; Michalak, R. S.; Nilakantan, R.; Discifani, C.; Golas, J.; Rabindran, S. K.; Shen, R.; Shi, X.; Wang, Y.; Upeslaci, J.; Wissner, A. *J. Med. Chem.* **2005**, *48*, 1107.
- Ram, S.; Wise, D. S.; Townsend, L. B. *J. Heterocyclic Chem.* **1986**, *23*, 1109.
- Pal, M.; Subramanian, C. V.; Yeleswarapu, K. R. *Tetrahedron Lett.* **2003**, *44*, 8221.
- Mastalerz, H.; Chang, M.; Chen, P.; Dextraze, P.; Fink, B.; Gavai, A.; Goyal, B.; Han, W.; Johnson, W.; Langley, D.; Lee, F. Y.; Marathe, P.; Mathur, A.; Oppenheimer, S.; Ruediger, E.; Tarrant, J.; Tokarski, J. S.; Vite, G. D.; Vyas, D.

- M.; Wong, H.; Wong, T. W.; Zhang, H.; Zhang, G. *Bioorg. Med. Chem. Lett.* **2007**, *17*, 2036.
16. Cockerill, S.; Stubberfield, C.; Stables, J.; Carter, M.; Guntrip, S.; Smith, K.; MaKeown, S.; Shaw, R.; Topley, P.; Thomsen, L.; Affleck, K.; Jowett, A.; Hayes, D.; Willson, M.; Woollard, P.; Spalding, D. *Bioorg. Med. Chem. Lett.* **2001**, *11*, 1401.
 17. The reaction was incubated for 60 min at 30 °C for ErbB-2 in (60 mM Hepes pH 7.5, 3 mM magnesium chloride, 3 mM manganese chloride, 0.003 mM sodium vanadate, 1.2 mM DTT, 50 g/mL PEG 20,000, 0.001 mM ATP, 1.5 ng/mL biotinylated polyGluTyr and 0.2 μ Curies 33 P- γ -ATP) and for EGFR in (50 mM Tris pH 8.0, 10 mM manganese chloride, 0.1 mM sodium vanadate, 1 mM DTT, 0.005 mM ATP, 1.5 ng/mL biotinylated polyGluTyr and 0.2 μ Curies 33 P- γ -ATP) in streptavidin coated FlashPlates (NEN, Boston, MA). Plates were sealed and read on the TopCount scintillation counter. Each measurement was performed at least in duplicate and the IC₅₀ values were calculated with standard deviation from 2 to 8 separate experiments.
 18. (a) Bhattacharya, S. K.; Cox, E. D.; Kath, J. C.; Mathiowetz, A. M.; Morris, J.; Moyer, J. D.; Pustilnik, L. R.; Rafidi, K.; Richter, D. T.; Su, C.; Wessel, M. D. *Biochem. Biophys. Res. Commun.* **2003**, *307*, 267; (b) Brignola, P. S.; Lackey, K.; Kadwell, S. H.; Hoffman, C.; Horne, E.; Carter, H. L.; Stuart, J. D.; Blackburn, K.; Moyer, M. B.; Alligood, K. J.; Knight, W. B.; Wood, E. R. *J. Bio. Chem.* **2002**, *277*, 1576.
 19. Antiproliferative activity of dual EGFR/ErbB-2 kinase inhibitors was assessed in monolayer cultures by 14 C-thymidine incorporation into cellular DNA as described Emanuel, S. et al *Mol. Pharm.* **2004**, *66*, 635. except that total time in which cells were exposed to drug was 96 h.
 20. Upstate Cell Signaling Solutions, Charlottesville, VA.
 21. (a) PDB code is 3BEL; (b) EGFR cloning. The DNA sequence encoding amino acids S671–G998 of human EGFR mature protein (Genbank Accession #NM 005228) was amplified by polymerase chain reaction (PCR) and inserted into the vector pDEST8 (Invitrogen) modified to include sequences encoding an in-frame hexameric histidine sequence and a thrombin cleavage site. The resulting construct thus encoded MHHHHHHVDLVPGRSHMA-(EGFR^{S671–G998}) which was confirmed by DNA sequencing. This expression construct was then integrated into bacmid DNA and a recombinant isolate used to transfect Sf9 insect cells as recommended by the vendor. The resulting baculovirus was then used to infect additional Sf9 cells to increase viral titer and volume; (c) EGFR purification. All purification processes were carried out on an ÄKTA FPLC system (GE Healthcare) at 4 °C. The purification protocol was performed as described previously [J. Biol. Chem. (2002), *277*, p. 46265–46272]. Briefly, frozen cells were thawed and resuspended in 50 mM Tris pH 7.5, 200 mM NaCl, 1% glycerol, 5 mM BME, 1 X complete EDTA-free protease inhibitor cocktail (Roche). Resuspended cells were dounce homogenized and mechanically lysed with an Emulsiflex-C5 (Avestin) at 10,000–15,000 psi. The lysate was clarified by centrifugation at 40,000g for 1 h. The supernatant was filtered through a 0.8 μ m vacuum filter and mixed to a TALON metal affinity resin (BD Biosciences) overnight at 4 °C. The lysate-TALON mixture was loaded into a column and washed with 10 column volumes of Buffer A (50 mM Tris pH 8.0, 500 mM NaCl, 5 mM imidazole.) EGFR was eluted using a 10 column volume linear gradient going from Buffer A to Buffer B (50 mM Tris pH 8.0, 300 mM NaCl, 250 mM Imidazole.) Fractions containing EGFR, as assayed by SDS–PAGE, were pooled. Thrombin was added to the pooled protein to remove the histidine tag (0.005 U of thrombin/ μ g EGFR). The reaction was dialyzed overnight against 50 mM Tris buffer pH 8.0, 250 mM NaCl, 1 mM DTT. Cleaved EGFR was filtered through a 0.2 μ m SPCA cartridge filter, concentrated, and loaded onto a Superdex 200 HR 10/30 column (GE Healthcare,) preequilibrated with 50 mM Tris pH 8.0, 500 mM NaCl, 1 mM DTT. Fractions containing EGFR, as assayed by SDS–PAGE, were pooled and dialyzed against 10 mM Tris pH 8.0, 1 mM DTT, 1 mM sodium azide, 0.1 mM benzamidine.; (d) Crystallization, data collection, molecular replacement, and structure refinement of the EGFR-compound **37** complex. Purified human EGFR was concentrated to 4 mg/ml, complex with compound **37** in a 1:2 ratio and crystallized from a solution containing 2 M Na/K₂PO₄, 0.1 M Caps pH 9.0 and 0.2 M Li₂SO₄.¹⁶ X-ray diffraction data to a resolution of 2.0 Å were collected at the IMCA-CAT ID-17 beamline at the Argonne National Laboratory. Diffraction data were indexed, integrated, and scaled using the HKL2000 suite. The EGFR crystals belong to the P212121 space group, with unit cell parameters $a = 45.50$, $b = 67.69$, $c = 103.25$ Å. The structure was determined by molecular replacement with CNX [Brunger, A. T., Adams, P. D., Clore, G. M., DeLano, W. L., Gros, P., Grosse-Kunstleve, R. W., Jiang, J. S., Kuszewski, J., Nilges, M., Pannu, N. S., Read, R. J., Rice, L. M., Simonson, T., Warren, G. L. (1998) *Acta Crystallogr D* *54*, 905–921] using the structure of EGFR complexed with Lapatinib as a search model (PDB id 1XKK).¹⁶ All model building was done using O [Jones, T. A., Zou, J. Y., Cowan, S. W., Kjeldgaard, M. (1991) *Acta Crystallogr A* *47*, 110–119] and refinement and map calculations were carried out using CNX [Brunger, A. T., Adams, P. D., Clore, G. M., DeLano, W. L., Gros, P., Grosse-Kunstleve, R. W., Jiang, J. S., Kuszewski, J., Nilges, M., Pannu, N. S., Read, R. J., Rice, L. M., Simonson, T., Warren, G. L. (1998) *Acta Crystallogr D* *54*, 905–921]. The final structure was refined to an Rfactor of 22.7 and Rfree of 26.7.
 22. Rusnak, D. W.; Affleck, K.; Cockerill, S. G.; Stubberfield, C.; Harris, R.; Page, M.; Smith, K. J.; Guntrip, S. B.; Carter, M. C.; Shaw, R. J.; Jowett, A.; Stables, J.; Topley, P.; Wood, E. R.; Brignola, P. S.; Kadwell, S. H.; Reep, B. R.; Mullin, R. J.; Alligood, K. J.; Keith, B. R.; Crosby, R. M.; Murray, D. M.; Knight, W. B.; Gilmer, T. M.; Lackey, K. *Cancer Res.* **2001**, *61*, 7196.
 23. Gaul, M. D.; Guo, Y.; Affleck, K.; Cockerill, G. S.; Gilmer, T. M.; Griffin, R. J.; Guntrip, S.; Keith, B. R.; Knight, W. B.; Mullin, R. J.; Murray, D. M.; Rusnak, D. W.; Smith, K.; Tadepalli, S.; Wood, E. R.; Lackey, K. *Bioorg. Med. Chem. Lett.* **2003**, *13*, 637.